Hindawi
Advances in Materials Science and Engineering
Volume 2023, Article ID 8888248, 10 pages
https://doi.org/10.1155/2023/8888248

Research Article

Adhesion of Nano-ZnO Modified Asphalt and Its Influence on Moisture-Sensitive Properties of Mixtures

Xiaoming Chen,[1] Ping Wen,[1] Qibin Ji,[1] Shujiang Jiang,[1] Zhimin Zhou,[1] Aipeng Wang,[2] Lingyun Li,[3] and Bowen Guan[2]

[1]*Chengdu Engineering Co.,Ltd. of China Railway 5 Bureau Group Corporation, Chengdu 610073, China*
[2]*School of Materials Science and Engineering, Chang'an University, Xi'an 710061, China*
[3]*Qinghai Traffic Investment Co.,Ltd., Xining 810000, China*

Correspondence should be addressed to Bowen Guan; bguan@chd.edu.cn

Received 25 November 2022; Revised 23 December 2022; Accepted 31 March 2023; Published 19 April 2023

Academic Editor: Meng Guo

This study investigates the effect of nano-ZnO on modified asphalt's adhesion characteristics by preparing various mixtures with 0%, 1%, 2%, and 3% nano-ZnO contents. Within the study context, the adhesion characteristics of asphalt mixtures with different nano-ZnO to limestone, basalt, and granite contents are studied using a boiling test. The surface-free energy (SFE) parameters of four asphalt and three aggregate types are evaluated using a theoretical approach and then verified by performing pull-off tests, and the adhesion work between different asphalt and aggregates is calculated. In addition, the effect of nano-ZnO on moisture-sensitive properties of the asphalt mixture is assessed using a freeze-thaw split test and semicircle bending (SCB) test. The study results have shown that nano-ZnO can enhance adhesion characteristics of the asphalt. The surface energy of modified asphalt with high ZnO content is relatively larger, and the adhesion between asphalt and limestone is better than the basalt and granite. The aggregates' chemical composition and the SFE's parameters significantly affect the adhesion between asphalt and aggregates. Furthermore, the correlation between the surface-free energy theory and the pull-off test results is better than the boiling test ones. Nano-ZnO enhances the asphalt mixture's moisture sensitivity before and after freeze-thaw cycles and impacts the initial state's tensile strength and cracks resistance, especially after freeze-thaw cycles where the improvement is obvious.

1. Introduction

Asphalt, a by-product of crude oil extraction, is widely used in pavement construction due to its excellent adhesion properties. Nowadays, most high-grade pavements worldwide are constructed using asphalt mixtures due to their low noise and comfort [1, 2]. However, when the asphalt is immersed in water, aggregates are prone to fall off, which seriously deteriorates the pavements and reduces their serviceability life. As a result, the road's maintenance cost increases, and driving comfort significantly reduces, causing traffic safety risks.

Previous researchers adopted various techniques that increase the adhesion between asphalt and aggregate, preventing asphalt pavement water damage and extending its service life [3, 4]. Some scholars have conducted molecular dynamic simulation analyses of recycled oil, carbon nanotubes, and other components and found that these additives can enhance the adhesion between asphalt and aggregates [5]. Liu et al. [6] performed a molecular dynamic simulation analysis on steel slag mineral components and found that the essential solid components in steel slag minerals enhance the adhesion with asphalt. Other scholars have found that the compatibility and adhesion performance can be improved using thermoplastic-modified asphalt treated with maleic anhydride [7]. Nevertheless, improving the direct adhesion between asphalt and aggregates is a complex issue.

The direct adhesion between asphalt and aggregate is affected by many factors, including asphalt aging, aggregate lithology, aggregate roughness, and temperature influence

[8–10]. Therefore, studying the adhesion between asphalt and aggregates is a multiscale method that includes the asphalt mixture's macroscopic mechanical strength, boiling test, water immersion test, pull-off strength of asphalt and aggregates, surface-free energy theory of asphalt and aggregates, and nanoscale atomic force microscope (AFM) observation and molecular dynamics simulation. The results of traditional boiling and water immersion tests are greatly affected by the investigators' subjectivity since it is a semiquantitative analysis that cannot quantitatively evaluate the adhesion between asphalt and aggregates. Some scholars have studied the influence of hydrated lime (HL) on the adhesion of asphalt, developed asphalt-aggregate adhesion failure model based on the surface-free energy (SFE) method, and found that the surface-free energy theory can explain the asphalt and aggregate adhesion to a good extent [11]. Lv et al. [12, 13] experimentally found that SBS, polyethylene, and rubber powder negatively affect modified asphalt's adhesion properties. Some scholars have used AFM observations to find that graphene oxide can change asphalt microstructure and enhance asphalt-aggregate adhesion [14, 15]. Incorporating an antistripping agent can significantly improve the adhesion between asphalt and aggregate while affecting the project cost [16, 17]. Generally, traditional polymer-modified asphalt is considered expensive, complex, and nonenvironmentally friendly. In contrast, nanomineral-modified asphalt is cheap, easy to process, and has low resource consumption, which meets the current green development requirements [18, 19].

Studies have indicated that interfacial water alters asphalt binders' nanostructure, making it a new way of improving the adhesion between asphalt and aggregate [20]. Jin et al. [21] found that nano-organic palygorskite and SBS composite-modified asphalt can effectively improve asphalt's adhesion performance. Furthermore, nano-SiO_2 can reduce the asphalt mixture's sensitivity to moisture damage and improve the antioxidative aging ability of the asphalt binder [22]. Moreover, adding nano-SiO_2 to the asphalt mixture after freeze-thaw cycles enhances its brittleness, fracture energy, and fracture toughness compared to conventional samples [23–25]. Additionally, nano-zinc oxide (ZnO) and nano-reduced graphene oxide (RGO) improves the antimoisture sensitivity of the stone mastic asphalt (SMA) mixture [26].

Therefore, this article studies the adhesion properties of nano-ZnO modified asphalt and three kinds of aggregates. The adhesion properties of nano-ZnO modified asphalt with limestone, basalt, and granite aggregates are comprehensively evaluated by the water boiling test, SFE theory, and pull-off test. In addition, the moisture-sensitive performance of different nano-ZnO-modified asphalt mixtures is assessed by conducting freeze-thaw split and semicircle bending (SCB) tests. The research results provide a reference for future nano-ZnO-modified asphalt utilizations.

2. Materials and Testing Methods

2.1. Materials. Table 1 provides the properties of the SK-90 asphalt used in this work, and Figure 1 shows 8000 times magnified microscopic image of the nano-ZnO utilized herein. The particle size of nano-ZnO is 30 nm, the purity is more than 99.8%, and the loss on ignition is less than 0.1%. The aggregate slabs are limestone, basalt, and granite, with the properties given in Table 2, and the XRF results are shown in Table 3. In general, distilled water, ethylene glycol, and glycerol were used to measure the contact angles of the asphalt and aggregates, and the surface energies of these liquids are shown in Table 4.

Table 1: Properties of the original asphalt.

Properties	Test results	Test methods [27]
Penetration (25°C, 100 g, 5 s; 0.1 mm)	88	T0604
Ductility (15°C, 5 cm/min; cm)	>100	T0605
Softening point (°C)	47.5	T0606
Density (g/cm^3)	1.011	T0603
Flash point (°C)	295	T0611

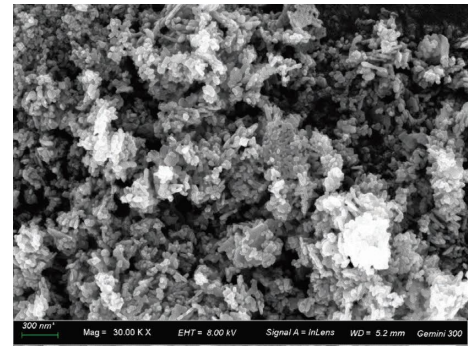

Figure 1: Micromorphology of nano-ZnO.

2.2. Preparation of Nano-ZnO Modified Asphalt. The nano-ZnO-modified asphalt used in this study was prepared through a high-speed shearing method. In this context, the asphalt was first heated to a molten state at 160°C, and nano-ZnO was gradually added, stirred manually for 10 min, and then sheared at 4000 rpm and 160°C for 60 min. The nano-ZnO dosages utilized herein are 1%, 2%, and 3%.

2.3. Asphalt Mixture Design. The optimal asphalt-aggregate ratio of the AC-13 mixtures was determined as 4.6% using the Marshall test. The aggregate gradation of the asphalt mixture used herein is shown in Table 5. Limestone was used as aggregates and asphalt contained 0%, 1%, 2%, and 3% nano-ZnO.

2.4. Methods

2.4.1. DSR Test. The dynamic shear rheometer (DSR) was used to test the rheological properties of asphalt mortars with different nano-ZnO contents. The test temperature ranged between 46°C and 70°C with 6°C interval, 10 rad/s frequency, and 1% strain control.

2.4.2. Boiling Test. In this study, the boiling test was performed based on the JTGE20-2011 specification [27], and the adhesion grades of different asphalt and aggregates were

Table 2: Properties of aggregates.

Aggregate type	Apparent density (kg·m^{-3})	Los Angeles abrasion (%)	Crushing value (%)	Water absorption (%)
Limestone	2.69	17.6	13.6	0.68
Basalt	2.73	15.8	12.9	0.59
Granite	2.72	15.9	12.5	0.62

Table 3: Chemical properties of aggregates.

Type	Chemical composition (wt%)										
	SiO_2	TiO_2	Al_2O_3	Fe_2O_3	MnO	MgO	CaO	Na_2O	K_2O	P_2O_5	LOI
Limestone	3.68	—	0.31	0.21	0.00	1.62	53.87	0.17	0.05	0.01	40.06
Basalt	42.69	3.21	13.95	12.11	0.18	7.61	10.23	3.87	2.92	1.14	2.09
Granite	71.95	0.10	14.58	0.82	0.02	0.75	1.42	3.99	5.11	0.03	1.23

Table 4: Surface-free energy components of reagent.

Reagent	γ (mJ/m^2)	γ^d (mJ/m^2)	γ^p (mJ/m^2)
Distilled water	72.8	21.8	51.0
Glycerin	64.0	34.0	30.0
Formamide	57.9	38.9	19.0

Table 5: Mix proportion for Marshall specimens.

Replacement (%)	Sieve size (mm)									
	0.075	0.15	0.3	0.6	1.18	2.36	4.75	9.5	13.2	16
Used	6	10	13.5	19	26.5	37	53	76.5	95	100
Upper limit	8	15	20	28	38	50	68	85	100	100
Lower limit	4	5	7	10	15	24	38	68	90	100

evaluated by extending the boiling time to 15 min. The test was conducted by three staff members, with the majority result prevailing in case the test results were inconsistent. Adhesion grades 5, 4, 3, 2, and 1 represent that the percentage of the asphalt spalled area is close to 0%, less than 10%, less than 30%, greater than 30%, and bare, respectively.

2.4.3. Surface-Free Energy Theory. The surface energy theory is often used to quantitatively evaluate the adhesion properties of asphalt to aggregates [28]. The governing expression for this theory is shown in the following equation:

$$\gamma = \gamma^d + \gamma^p, \tag{1}$$

where γ is the surface energy (mJ/m^2); γ^d is the dispersion component (mJ/m^2); γ^p is the polar component (mJ/m^2).

Asphalt's surface energy parameters can be calculated using equations (2) to (4):

$$\gamma_l \cos\theta = \gamma_s - \gamma_{sl}, \tag{2}$$

$$\gamma_{sl} = \gamma_s + \gamma_l - 2\sqrt{\gamma_s^d \gamma_l^d} - 2\sqrt{\gamma_s^p \gamma_l^p}, \tag{3}$$

$$\frac{1+\cos\theta}{2}\frac{\gamma_l}{\sqrt{\gamma_l^d}} = \sqrt{\gamma_l^p}\sqrt{\frac{\gamma_l^p}{\gamma_l^d}} + \sqrt{\gamma_s^d}, \tag{4}$$

where γ_s, γ_l, and γ_{sl} are the surface energy (mJ/m^2) of the solid, liquid, and solid-liquid interface, respectively; γ_l^d and γ_l^p are the dispersive and polar components (mJ/m^2) of the liquid, respectively; γ_s^d and γ_s^p are the dispersion component and polar component of solid (asphalt) (mJ/m^2); θ is the angle connecting the solid-liquid interface.

Generally, the adhesion work is used to evaluate the difficulty of water penetrating the binder-aggregate interface of the asphalt mixture. Furthermore, the adhesion work of the asphalt-aggregate system can be calculated using the following equation:

$$W_{as} = \gamma_l (1 + \cos\theta), \tag{5}$$

where W_{as} is the adhesive work between the asphalt and aggregate (mJ/m^2).

In the actual measurement, the actual heating temperature, drop height, and droplet size of asphalt are difficult to control. Accordingly, equation (6) is typically used to calculate the asphalt-aggregate adhesion work.

$$W_{as} = 2\left(\sqrt{\gamma_s^d \gamma_a^d} + \sqrt{\gamma_s^p \gamma_a^p}\right), \tag{6}$$

where γ_s^d and γ_s^p are the dispersion and polar components of the solid's surface energy (mJ/m^2), respectively; γ_a^d and γ_a^p are the dispersion and polar components of asphalt (mJ/m^2), respectively.

2.4.4. Contact Angle Test. Distilled water, ethylene glycol, and glycerol, with known surface energy parameters, were used to quantify the surface-free energy of asphalt film samples. Moreover, the aggregate's contact angle was measured using three probe liquids, and the aggregate's surface-free energy parameter was calculated according to the above surface energy theory. Before the aggregate contact angle test, one aggregate sheet side was treated with 1500 mesh sandpaper to avoid errors caused by the aggregate's rough surface. Moreover, a contact angle tester was used, and 25°C temperature was maintained during the experiment.

2.4.5. Pull-Off Test. A pull-off test was used to evaluate the adhesion between asphalt and different aggregates. The testing procedure started by putting asphalt, aggregate slabs, and drawing heads into the oven at 165°C to melt and flow the asphalt and fully dry the aggregate slabs and drawing heads. Thereafter, different asphalts were dropped on the aggregate slabs, and the asphalt film thickness was controlled at 0.2 mm. After 24 h of molding, a Defeleko Positest AT-A machine was used to test the maximum strength of each mixture at 25°C. In general, three parallel tests were carried out for each case.

2.4.6. Freeze-Thaw Split Test. The freeze-thaw splitting test was carried out on asphalt mixtures with different nano-ZnO contents based on the specification JTG E20-2011 [27]. In this context, standard Marshall Specimens were saturated with water under a vacuum for 15 min and then soaked under normal pressure for 30 min. After that, the samples were put into plastic bags with 10 ml of water and frozen in a −20°C incubator for 16 h. Thereafter, the samples were dissolved in a 60°C constant temperature water tank for a range of 4 h freeze-thaw cycles. Finally, the unfreeze-thawed and frozen-thawed specimens were loaded until failure, and the tensile strength ratio (TSR) was calculated according to equations (7) to (9):

$$R_{T1} = 0.006287 \frac{P_{T1}}{h_1}, \tag{7}$$

$$R_{T2} = 0.006287 \frac{P_{T2}}{h_2}, \tag{8}$$

$$\mathrm{TSR} = \frac{\overline{R}_{T2}}{\overline{R}_{T1}} \times 100, \tag{9}$$

where TSR is the tensile strength ratio (%); R_{T1} is the average tensile strength (MPa) of the unconditioned specimen; R_{T2} is the average tensile strength (MPa) of the conditioned specimen; P_{T1} is the maximum value of test load for the test pieces in the first group (N); P_{T2} is the maximum value of the test load for the test pieces in the second group (N).

2.4.7. Semicircle Bending (SCB) Test. The semicircle bending (SCB) test has the advantages of a simple test method and reliable test data. It is often used for testing asphalt mixture performance [29]. The SCB specimens used in this work were obtained from standard Marshall Specimens with 25 mm thickness. A 3 mm × 15 mm presplit was cut in the center of the SCB specimen to induce the crack development there. Before the test, the SCB samples were cooled at −15°C for 4 h to avoid creep instability. The SCB specimens were supported in the bottom at 80 mm intervals during the test, and the upper center was lowered at a rate of 0.5 mm/min to apply the load until the specimen was broken, as shown in Figure 2. The maximum load was recorded to evaluate the mechanical properties of the asphalt mixture.

In order to study the effect of moisture on the peak fracture load of SCB samples, the SCB samples were divided into conditioned and unconditioned groups, and the samples in the conditioned group were subjected to freeze-thaw cycles before testing. The load rate was defined as the ratio of the conditioned sample's peak loading to the unconditioned one.

3. Results and Discussion

3.1. Analysis of Nano-ZnO Modified Asphalt

3.1.1. Rheological Results. Figure 3 shows the variation in the rutting factor of asphalt with different nano-ZnO contents under induced temperature. The rutting factor can reflect the ability of asphalt to resist permanent deformation under high-temperature conditions. It gradually decreases with the increase in temperature, while nano-ZnO can increase the rutting factor of asphalt under the same conditions, leading to asphalt hardening. In other words, nano-ZnO helps improve the asphalt's high-temperature rheological properties due to its physical properties.

By taking the rutting factors of different asphalt mixtures at 58°C as an example, it can be seen that the rutting factors ZnO-1%, ZnO-2%, and ZnO-3% cases were increased by 8.45%, 31.13%, and 35.95%, respectively, compared to the control mixture. The above results show that the improvement in the nano-ZnO asphalt's rutting factor is different from that of the content of nano-ZnO due to the nano-ZnO uneven dispersion.

Figure 4 shows the variation in the phase angle of four pitches with different nano-ZnO contents at 46–70°C. The phase angle and viscosity of conventional asphalt gradually increase with the temperature rise. However, unlike the control case, the phase angle of asphalt containing nano-ZnO only increases to a certain extent between 46 and 58°C, and then the phase angle gradually decreases, approaching 75° at 70°C. This is mainly caused by the nano-ZnO's physical characteristics. Nano-ZnO has an agglomeration effect on the asphalt mixture, which affects its dispersion uniformity.

3.1.2. Boiling Results. Figure 5 shows the boiling test results for the four asphalt and three aggregate types. It can be seen that the adhesion performance of the four asphalt mixtures with limestone is the best; all are grade 4. On the other hand, the adhesion performance of the basalt-based ZnO-1% case is grade 3, while that of basalt-based ZnO-2% and ZnO-3% is

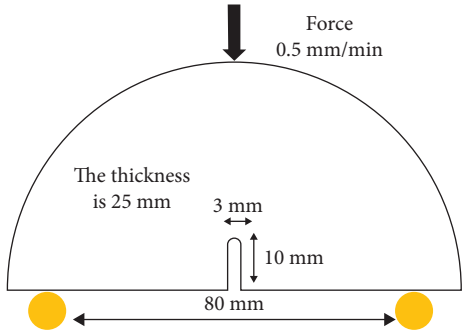

Figure 2: SCB test procedure.

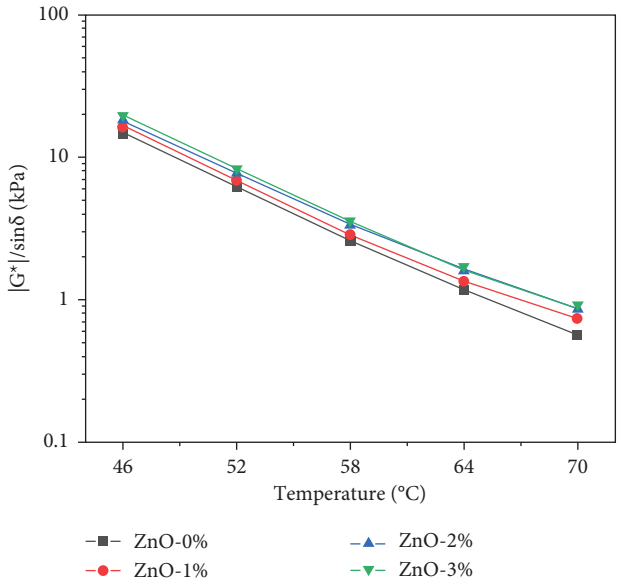

Figure 3: The rutting factor of different asphalt.

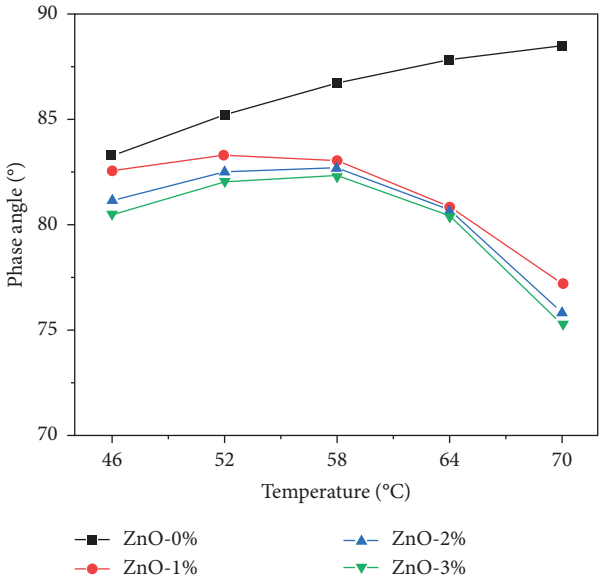

Figure 4: Phase angle of different asphalt.

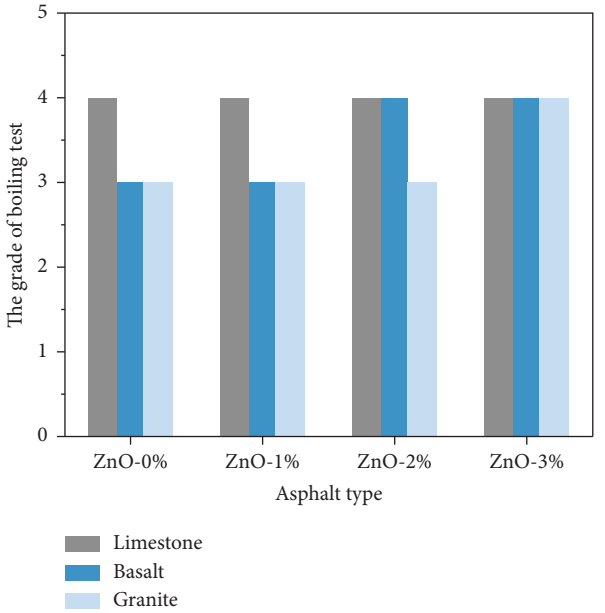

Figure 5: The results of the boiling test.

grade 4. Among granite-based mixtures, only the ZnO-3% case reached grade 4, whereas the rest were grade 3. It is worth noting that the results of the boiling test are greatly affected by the evaluator's subjectivity, but in this work, three testers evaluate the results simultaneously to get reliable results.

It can be seen from the boiling results that the adhesion between limestone and asphalt is the best, followed by basalt and then granite. This is mainly determined using different lithologic aggregates' chemical composition and surface roughness. Nano-ZnO can considerably improve asphalt's adhesion performance. Nevertheless, solely performing a boiling test is not enough to show this improvement.

3.1.3. Analysis of Surface Energy Results of Modified Asphalt. Figure 6 shows the calculation results of the surface energy parameters for four different asphalts. It can be seen that the polar components of the four cases are all much smaller than the dispersion ones. However, they have slight differences. The pitch's dispersive component and total surface energy increased gradually with the increase in the nano-ZnO content, with the total surface energy ranging from 16 mJ/m^2 to 20 mJ/m^2. The surface energy theory states that the surface energy of a substance in a stable state is low. Thus, asphalts with high surface energy adhere strongly. Based on the surface energy parameters of the control asphalt and the three nano-ZnO-modified cases, it can be seen that the ZnO-3% has the highest value, followed by the ZnO-2% and then the ZnO-1% cases.

3.1.4. Analysis of Adhesion Work of Modified Asphalt and Aggregates. Table 6 shows the surface energy parameters' results for three aggregate types. The surface energy of

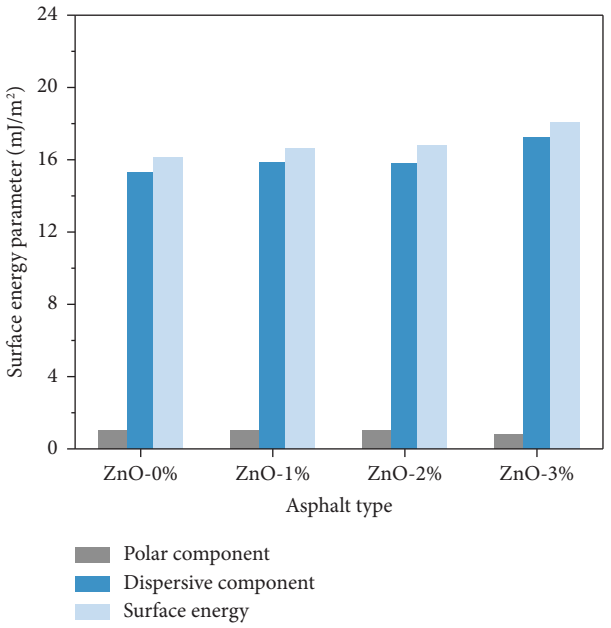

Figure 6: Surface energy parameters of different asphalt.

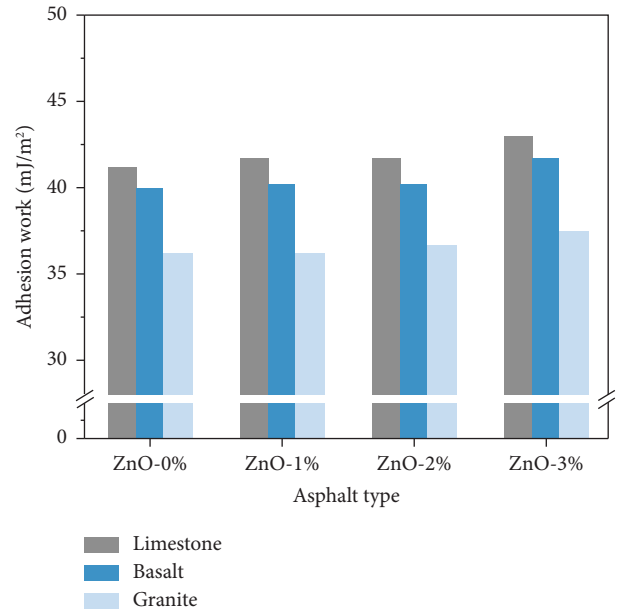

Figure 7: Adhesion work of different asphalt and three aggregates.

Table 6: Surface-free energy components of aggregates.

Aggregate type	γ^d (mJ/m^2)	γ^p (mJ/m^2)	γ (mJ/m^2)
Limestone	52.17	1.29	53.46
Basalt	50.31	0.86	51.17
Granite	44.23	3.68	47.91

limestone is greater than that of basalt, while that of granite is the smallest. The polar components of the three aggregates are all small, especially limestone and basalt, which are below 1.3 mJ/m^2, while the polar component of granite is 3.68 mJ/m^2, reflecting strong granite polarity.

Figure 7 shows the calculated adhesion work for different asphalts and aggregates. It can be noticed that the four asphalts have the highest adhesion to limestone, followed by basalt, and then granite. By taking the control asphalt as an example, the adhesion work of limestone, basalt, and granite are 41.11 mJ/m^2, 39.81 mJ/m^2, and 36.07 mJ/m^2, respectively. This trend is consistent with the boiling test. In addition, from the perspective of asphalt, incorporating nano-ZnO increases the adhesion work between the modified asphalt and aggregate, thereby enhancing the adhesion performance. By taking the basalt as an example, the adhesion work of ZnO-0%, ZnO-1%, ZnO-2%, and ZnO-3% are 39.81 mJ/m^2, 40.18 mJ/m^2, 40.37 mJ/m^2, and 41.70 mJ/m^2, respectively. Hence, the adhesion work of ZnO-1% modified asphalt and ZnO-2% modified asphalt show slight improvement over the control case, while that of ZnO-3% has more than 4.7% increase compared to the base asphalt. This is due to the large surface area of the nano-ZnO, which absorbs part of the light components in the asphalt, thereby increasing the adhesion work between the modified asphalt and aggregates.

3.1.5. Analysis of Pull-Off Test Results. The tensile strength results of different asphalt and aggregates are shown in Figure 8. The pull-off strength increases with the increase in the ZnO content, and the pull-off strength with limestone is the highest, followed by basalt and then granite. This pattern is consistent with the test results of the surface energy and the calculation results of the adhesion work between the aggregates. As an acidic substance, the adhesion between asphalt and aggregates is greatly affected by the acidity and alkalinity of aggregates. It can be seen from Table 3 that the SiO_2 content of granite is 71.95%, which is regarded as acid aggregate. The SiO_2 content of limestone is 3.68%, which is regarded as an alkaline aggregate, and the SiO_2 content of basalt is 42.69%. The adhesion between alkaline aggregate and asphalt is better than that of acid aggregate.

3.2. Analysis of Nano-ZnO-Modified Asphalt Mixture

3.2.1. Freeze-Thaw Split Test Results. Figure 9 shows the freeze-thaw split test results of the asphalt mixture containing different nano-ZnO content. Figure 9(a) depicts the tensile strength results of different samples before and after freeze-thaw cycles. It can be noticed that nano-ZnO can increase the tensile strength of asphalt mixture regardless of whether freeze-thaw cycles are performed. From the perspective of unconditioned samples, 1%, 2%, and 3% nano-ZnO can increase the strength by 7.7%, 10.9%, and 14.9%, respectively, compared to the conventional samples. On the other hand, from the perspective of conditioned samples, incorporating 1%, 2%, and 3% nano-ZnO increases the strength by 20.9%, 26.4%, and 31.6%, respectively. As shown in Figure 9(b), the TSR changes of different asphalt mixtures are also different. For instance, the TSR of the conventional

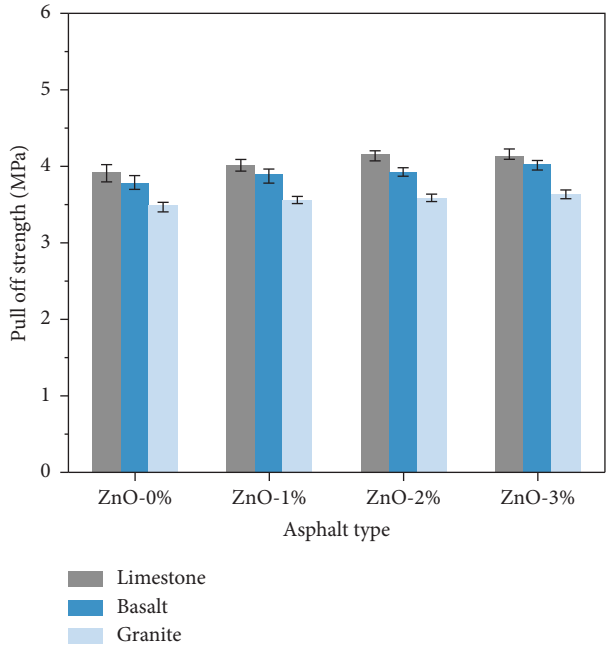

Figure 8: Pull-off strength of different asphalt and three aggregates.

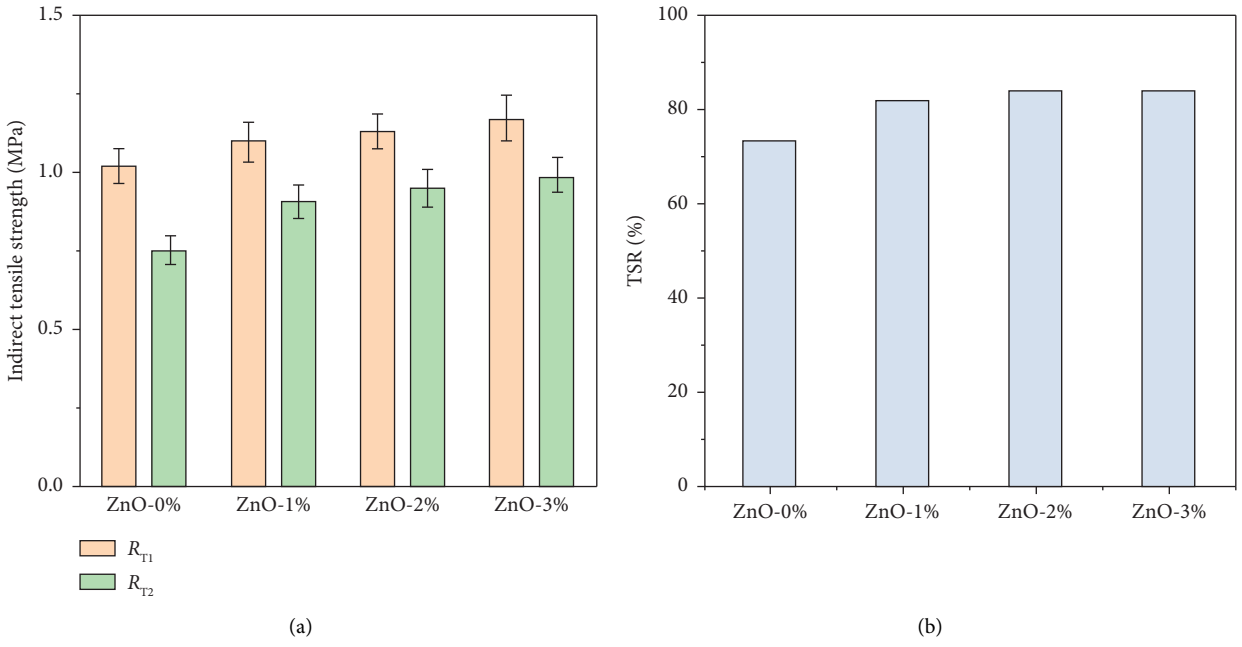

Figure 9: Freeze-thaw split test results: (a) indirect tensile strength and (b) TSR.

sample is 73.6%, while that of the samples containing nano-ZnO is more than 80%. The presence of water or ice in the mixture during freeze-thaw cycles decreases asphalt-aggregate adhesion, so the strength of the treated sample is low. Moreover, nano-ZnO significantly affects the adhesion performance of asphalt and aggregate in the mixture due to bond loss between asphalt and aggregate at the nanoscale. Nevertheless, nanomaterials can prevent this problem.

3.2.2. SCB Test Results. Figure 10(a) shows the peak load comparison results of asphalt mixtures containing nano-ZnO before and after the freeze-thaw treatment. In general, the peak load of different asphalt mixtures increases with the increase in the nano-ZnO content. Accordingly, nano-ZnO improves the fracture resistance of the asphalt mixture, thereby enhancing its flexibility. During the freeze-thaw cycle, the freezing and expansion of water in the voids lead to the formation and expansion of microcracks,

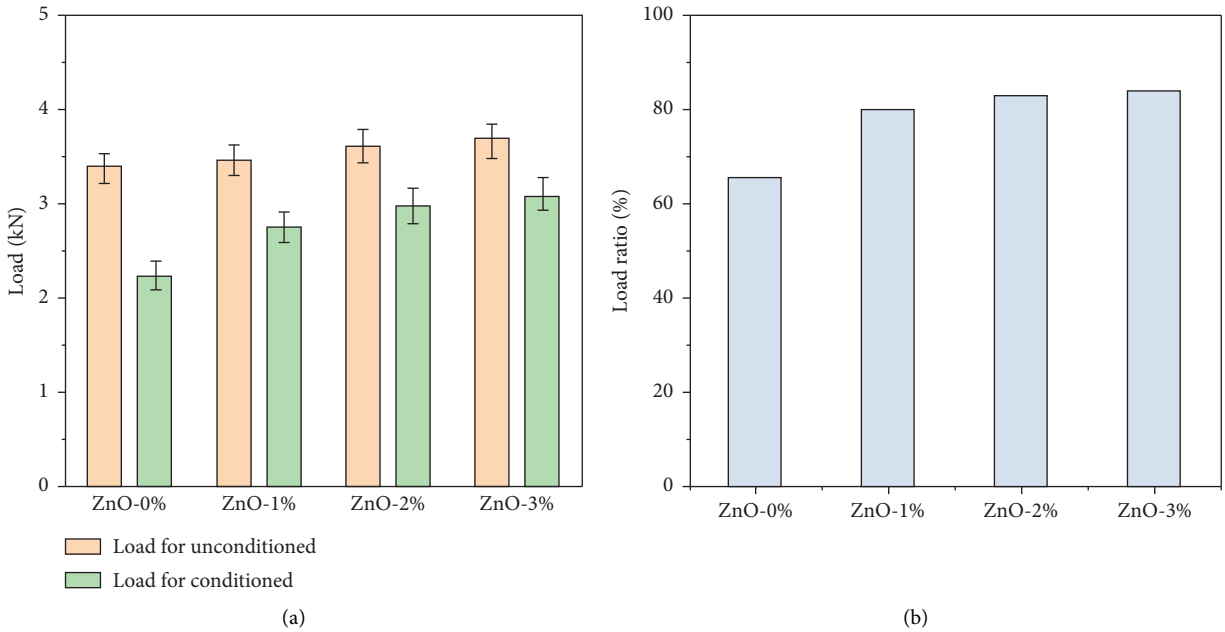

Figure 10: SCB test results: (a) load and (b) load ratio.

increasing the void ratio and reducing the adhesion force between aggregate and asphalt. In contrast, the loading of the samples containing nano-ZnO in the conditioned state is significantly higher than that of the control samples. Moreover, asphalt mixtures containing 1%, 2%, and 3% nano-ZnO increase the load by 23.8%, 33.3%, and 39.2%, respectively.

Figure 10(b) shows the loading ratio of different mixtures before and after freezing and thawing. It can be seen that the load ratio of the conventional sample is 66.2%, while that containing 1%, 2%, and 3% nano-ZnO is 79.2%, 82.6%, and 84.6%, respectively. Nano-ZnO prevents crack growth in the SCB test, and its high specific surface area increases the adhesion between asphalt and aggregates, thereby improving the mixture's resistance to fatigue crack growth [30]. In addition, interfacial tension is critical to the performance of asphalt-coated aggregate. Combined with the above analysis on the surface-free energy of nano-ZnO modified asphalt, nano-ZnO improves the contact between aggregate surface and asphalt by changing the interfacial tension, thus increasing the moisture resistance of the asphalt mixture [31].

4. Conclusion

This study investigates the adhesion performance of the nano-ZnO-modified asphalt with different aggregates and moisture sensitivities. Based on the aforementioned statements, the following conclusions are drawn:

(1) Nano-ZnO improves the adhesion performance of asphalt. The boiling test results showed that the adhesion of limestone-based asphalt mixtures is the best, followed by basalt and granite, due to the aggregates' chemical composition characteristics.

(2) Based on the SFE theory, the polar components of different asphalt are much smaller than the dispersion components. Moreover, the dispersion component and total surface energy of nano-ZnO modified asphalt gradually increased with the increase in the nano-ZnO content. The adhesion work of asphalt and limestone is the largest, which is consistent with the boiling experiment.

(3) The pull-off strength of asphalt and limestone is the highest, followed by basalt and granite. With the increase in the nano-ZnO content, the tensile strength between asphalt and aggregate increases, which was consistent with the SFE's theoretical results.

(4) Nano-ZnO improves the asphalt mixture's crack resistance. Furthermore, the freeze-thaw splitting test and SCB test results have good consistency. Especially, after freeze-thaw cycles, the moisture sensitivity of the asphalt mixture containing nano-ZnO has been improved.

(5) Nano-ZnO positively affects the adhesion properties of asphalt and its moisture sensitivity to the asphalt mixture. Combining the rheological parameters of nano-ZnO-modified asphalt and the residual strength of the mixture after freeze-thaw cycles, the optimal dosage of nano-ZnO is 2%.

(6) In the future, further research should be carried out on the dispersion uniformity of nano-ZnO and the feasibility of its application in asphalt mixtures. The improvement of asphalt adhesion performance by nano-ZnO should be further studied at the nanoscale.

Data Availability

The data used to support the findings of this study are included within the article.

Conflicts of Interest

The authors declare that they have no conflicts of interest.

Acknowledgments

This research was supported by the Key Research and Development and Transformation Plan of Qinghai Province (project no. 2021-SF-165) and Technology Achievement Transformation Project of Qinghai Province (project no. 2021-SF-140).

References

[1] J. Liu, L. Qi, X. Wang, M. Li, and Z. Wang, "Influence of aging induced by mutation in temperature on property and microstructure development of asphalt binders," *Construction and Building Materials*, vol. 319, Article ID 126083, 2022.

[2] J. Liu, Z. Wang, R. Luo, G. Bian, Q. Liang, and F. Yan, "Changes of components and rheological properties of bitumen under dynamic thermal aging," *Construction and Building Materials*, vol. 303, Article ID 124501, 2021.

[3] M. Guo, Y. Tan, and S. Zhou, "Multiscale test research on interfacial adhesion property of cold mix asphalt," *Construction and Building Materials*, vol. 68, pp. 769–776, 2014.

[4] J. Liu, Z. Wang, X. Zhao, C. Yu, and X. Zhou, "Quantitative evaluations on influences of aggregate surface texture on interfacial adhesion using 3D printing aggregate," *Construction and Building Materials*, vol. 328, Article ID 127022, 2022.

[5] M. Nikookar, M. Bagheri Movahhed, J. Ayoubinejad, V. Najafi Moghaddam Gilani, and S. M. Hosseinian, "Improving the moisture sensitivity of asphalt mixtures by simultaneous modification of asphalt binder and aggregates with carbon nanofiber and carbon nanotube," *Advances in Civil Engineering*, vol. 2021, Article ID 6682856, 11 pages, 2021.

[6] J. Liu, B. Yu, and Q. Hong, "Molecular dynamics simulation of distribution and adhesion of asphalt components on steel slag," *Construction and Building Materials*, vol. 255, Article ID 119332, 2020.

[7] S. Chen, T. Che, A. Mohseni, H. Azari, P. A. Heiden, and Z. You, "Preliminary study of modified asphalt binders with thermoplastics: the Rheology properties and interfacial adhesion between thermoplastics and asphalt binder," *Construction and Building Materials*, vol. 301, Article ID 124373, 2021.

[8] M. Nazirizad, A. Kavussi, and A. Abdi, "Evaluation of the effects of anti-stripping agents on the performance of asphalt mixtures," *Construction and Building Materials*, vol. 84, pp. 348–353, 2015.

[9] A. E. Alvarez, L. V. Espinosa, A. M. Perea, O. J. Reyes, and I. J. Paba, "Adhesion quality of chip seals: comparing and correlating the plate-stripping test, boiling-water test, and energy parameters from surface free energy," *Journal of Materials in Civil Engineering*, vol. 31, no. 3, 2019.

[10] A. A. Tayebali, A. Kusam, and C. Bacchi, "An innovative method for interpretation of asphalt boil test," *Journal of Testing and Evaluation*, vol. 46, no. 4, pp. 20160383–20161635, 2018.

[11] S. Han, S. Dong, M. Liu, X. Han, and Y. Liu, "Study on improvement of asphalt adhesion by hydrated lime based on surface free energy method," *Construction and Building Materials*, vol. 227, Article ID 116794, 2019.

[12] Q. Lv, W. Huang, N. Tang, and F. Xiao, "Comparison and relationship between indices for the characterization of the moisture resistance of asphalt-aggregate systems," *Construction and Building Materials*, vol. 168, pp. 580–589, 2018.

[13] L. Zhou, W. Huang, Y. Zhang, Q. Lv, and L. Sun, "Mechanical evaluation and mechanism analysis of the stripping resistance and healing performance of modified asphalt-basalt aggregate combinations," *Construction and Building Materials*, vol. 273, Article ID 121922, 2021.

[14] M. Guo, M. Liang, Y. Jiao, Y. Tan, J. Yu, and D. Luo, "Effect of aging and rejuvenation on adhesion properties of modified asphalt binder based on AFM," *Journal of Microscopy*, vol. 284, no. 3, pp. 244–255, 2021.

[15] X. Ji, J. Li, X. Zhai, H. Zou, and B. Chen, "Application of atomic force microscope to investigate the surface microadhesion properties of asphalt," *Materials*, vol. 13, no. 7, p. 1736, 2020.

[16] J. Liu, Z. Wang, M. Li, X. Wang, Z. Wang, and T. Zhang, "Microwave heating uniformity, road performance and internal void characteristics of steel slag asphalt mixtures," *Construction and Building Materials*, vol. 353, Article ID 129155, 2022.

[17] J. Liu, T. Zhang, H. Guo, Z. Wang, and X. Wang, "Evaluation of self-healing properties of asphalt mixture containing steel slag under microwave heating: mechanical, thermal transfer and voids microstructural characteristics," *Journal of Cleaner Production*, vol. 342, Article ID 130932, 2022.

[18] Z. Dai, J. Shen, P. Shi, X. Li, and H. Li, "Multi-scaled properties of asphalt binders extracted from weathered asphalt mixtures," *International Journal of Pavement Engineering*, vol. 21, no. 13, pp. 1651–1661, 2020.

[19] A. Azarhoosh, H. F. Abandansari, and G. H. Hamedi, "Surface-free energy and fatigue performance of hot-mix asphalt modified with nano lime," *Journal of Materials in Civil Engineering*, vol. 31, no. 9, 2019.

[20] W. Sun and H. Wang, "Moisture effect on nanostructure and adhesion energy of asphalt on aggregate surface: a molecular dynamics study," *Applied Surface Science*, vol. 510, Article ID 145435, 2020.

[21] J. Jin, Y. Gao, Y. Wu et al., "Rheological and adhesion properties of nano-organic palygorskite and linear SBS on the composite modified asphalt," *Powder Technology*, vol. 377, pp. 212–221, 2021.

[22] Z. Long, L. You, X. Tang, W. Ma, Y. Ding, and F. Xu, "Analysis of interfacial adhesion properties of nano-silica modified asphalt mixtures using molecular dynamics simulation," *Construction and Building Materials*, vol. 255, Article ID 119354, 2020.

[23] M. Zarei, A. Salehikalam, E. Tabasi, A. Naseri, M. Worya Khordehbinan, and M. Negahban, "Pure mode I fracture resistance of hot mix asphalt (HMA) containing nano-SiO2 under freeze-thaw damage (FTD)," *Construction and Building Materials*, vol. 351, Article ID 128757, 2022.

[24] J. Liu, Z. Wang, H. Guo, and F. Yan, "Thermal transfer characteristics of asphalt mixtures containing hot poured steel slag through microwave heating," *Journal of Cleaner Production*, vol. 308, Article ID 127225, 2021.

[25] D. Yu, H. Jing, and J. Liu, "Effects of freeze-thaw cycles on the internal voids structure of asphalt mixtures," *Materials*, vol. 15, no. 10, p. 3560, 2022.

[26] M. Fakhri and E. Shahryari, "The effects of nano zinc oxide (ZnO) and nano reduced graphene oxide (RGO) on moisture susceptibility property of stone mastic asphalt (SMA)," *Case Studies in Construction Materials*, vol. 15, p. 655, 2021.

[27] Jtg E20-2011, *Standard Test Methods of Bitumen and Bituminous Mixtures for Highway Engineering*, Ministry of Transport of the People's Republic of China, Beijing, China, 2011.

[28] X. Wang, J. Liu, Z. Wang, H. Jing, and B. Yang, "Investigations on adhesion characteristics between high-content Rubberized asphalt and aggregates," *Polymers*, vol. 14, no. 24, p. 5474, 2022.

[29] A. Kavussi, M. M. Karimi, and E. Ahmadi Dehaghi, "Effect of moisture and freeze-thaw damage on microwave healing of asphalt mixes," *Construction and Building Materials*, vol. 254, Article ID 119268, 2020.

[30] M. Fakhri and A. Rahimzadeh Mottahed, "Improving moisture and fracture resistance of warm mix asphalt containing RAP and nanoclay additive," *Construction and Building Materials*, vol. 272, Article ID 121900, 2021.

[31] G. H. Hamedi, F. M. Nejad, and K. Oveisi, "Estimating the moisture damage of asphalt mixture modified with nano zinc oxide," *Materials and Structures*, vol. 49, no. 4, pp. 1165–1174, 2016.